From Measurements to Models: Toward Accurate Representation of Brown Carbon in Climate Calculations

Rawad Saleh

Air Quality and Climate Research Laboratory, University of Georgia, 110 Riverbend Road, Athens, GA 30602, USA

School of Environmental, Civil, Agricultural, and Mechanical Engineering, University of Georgia, 597 D.W. Brooks Drive, Athens, GA 30602, USA

rawad@uga.edu, (706) 542-6110

Abstract

Purpose of review: The direct radiative effect of brown carbon (BrC) absorption predicated by climate-modeling studies is highly uncertain, with values ranging between +0.03 W/m^2 and +0.57 W/m^2. This review strives to identify sources of this uncertainty stemming from challenges in translating measurements into model inputs and to draw lessons from recent advances that lead to improved BrC representation in models.

Recent findings: Previously thought to absorb only short-visible and UV light, BrC was recently shown to comprise components that are strongly absorptive in the mid- and long-visible wavelengths, with light-absorption efficiencies approaching that of black carbon. The classic picture of biomass and biofuel combustion being the major sources of atmospheric BrC still holds, with recent measurements indicating a strong correlation between BrC optical properties and combustion conditions. Other combustion sources of BrC, currently not accounted for in models, include low-efficiency coal combustion and ship engines utilizing heavy fuel oil. Gas-phase, aqueous, and particle-phase reactions in the atmosphere produce secondary BrC and bleach/darken the primary BrC. Climate-modeling studies revealed that predicted BrC radiative effects are sensitive to the assumed optical properties and atmospheric aging mechanisms.

Summary: BrC can be grouped into four optical classes, each separated by an order of magnitude in mid-visible light absorption. The classes are approximately mapped to BrC sources, with secondary BrC being the least absorbing and BrC from high-temperature combustion the most absorbing. There is evidence that each class exhibits characteristic physicochemical properties (molecular size, volatility, solubility), which can be leveraged to design measurements that quantify distributions of BrC across classes as well as rates of photobleaching/darkening for each class. Utilizing this framework to develop BrC parameterizations promises to enhance its representation in climate models.

Keywords: brown carbon, black carbon, aerosol light absorption, refractive index, atmospheric aging, radiative effect

1. Introduction

In 1984, Patterson and McMahon [1] reported measurements of light-absorption properties of aerosols emitted from the flaming and smoldering phases of biomass fires. They found that black particles with strong absorption in the visible spectrum but weak wavelength dependence were emitted during the flaming phase, while the smoldering phase emitted yellow / light-brown particles with weak absorption but strong wavelength dependence. In another mid-1980s study, Mukai and Ambe [2] identified brown particles in the atmosphere with chemical signatures similar to humic acids, which they hypothesized to have originated from smoldering combustion of vegetation. The particles observed in these studies belong to the family of light-absorbing organic aerosols (OA) that we nowadays refer to collectively as brown carbon (BrC), a term coined by Andreae and Gelencsér [3]. The findings of these and other early pioneering studies [3] still largely shape the current perception of BrC: 1) produced during low-temperature pyrolysis or smoldering combustion of biomass fuels via formation pathways that are distinct from those of black carbon (BC), which is produced during high-temperature flaming combustion; 2) weakly / negligibly absorbing in the mid- and long-visible wavelengths but exhibits a sharp increase in absorption toward the short-visible and UV wavelengths; and 3) has chemical structure similar to humic-like substances (HULIS).

Recent evidence indicates that this picture of BrC is incomplete. Laboratory and field measurements of biomass and biofuel combustion have shown that the high-temperature BC-producing phase also produces BrC [4–9]. Some types of BrC were shown to be produced via the same soot-formation pathways that produce BC [10] and have molecular structures different from HULIS. Strongly absorbing BrC with light-absorption properties approaching those of BC (significant absorption in the mid- and long-visible wavelengths and relatively shallow wavelength dependence) was detected in laboratory and field measurements [8,10–15]. In addition to combustion, secondary reactions in the atmosphere were also found to be important sources of BrC [16,17]. BrC light absorption was shown to be dynamic, where BrC can undergo photobleaching [18–22] or darkening [23–25] as it evolves in the atmosphere.

Even though BrC was initially investigated (before it was called BrC) due to its effect on visibility [1], currently the main interest in BrC stems from its effect on climate as a particulate absorber of solar radiation alongside BC and mineral dust. Atmospheric observations revealed that BrC absorption in the short-visible and near-UV wavelengths rivals or exceeds BC in some regions [26,27]. Elucidating the radiative effect of BrC requires accurate representation in climate models, which in turn requires the development of frameworks that efficiently translate relevant BrC properties from measurements to models. This review strives to present an updated picture of BrC based on the recent advances outlined above with focus on practical implementation in climate models. It highlights challenges in the measurement and modeling realms and discusses means for addressing them. Section 2 presents a categorization of BrC into different classes based on their optical properties. It provides evidence that the optical classes are linked to BrC physicochemical properties (molecular size, volatility, solubility) and are correlated with BrC sources. Section 3 discusses recent findings on the evolution of BrC in the atmosphere. Section 4 summarizes the current implementations of BrC in climate models and discusses how the recent advances in measurements (Section 2 and Section 3) can potentially enhance the representation

of BrC in models. This review does not present a comprehensive survey of BrC physicochemical properties and speciation / optical-measurement techniques. There are excellent reviews that readers are referred to for this purpose [3,16,17,28].

2. Categorizing brown carbon

Unlike BC which has relatively uniform physicochemical and optical properties [29], BrC is a vast collection of species that are 1) light-absorbing in the visible and near-UV wavelengths and 2) organic [3]. The diversity in the chemical nature and molecular sizes of the BrC components is manifested as large variabilities in their volatility, solubility and, most importantly, optical properties [10,15]. In fact, some BrC components are optically more similar to BC than they are to other BrC components [10]. Representing BrC as a single species in climate models limits the ability to capture the range of effects this variability in BrC has on atmospheric radiation. On the other hand, similar to OA in general, a detailed representation of the BrC components in large-scale models is not only prohibitively expensive, but is also subject to limitations in the fundamental understanding of BrC. This section builds on recent advances in BrC measurements to propose a framework for representing the variability in BrC properties and highlights measurement needs to achieve this framework.

2.1. Brown carbon sources

The major source of atmospheric BrC is biomass combustion, including open-biomass and solid-biofuel combustion [7,26,30–32]. On the other hand, fossil-fuel combustion is not an important BrC emitter, with a few exceptions including low-efficiency residential-coal combustion [27,28,33] and heavy-fuel-oil (HFO) combustion in ship engines [15,34]. This should not be taken as an indication that the formation pathways of BrC are exclusively linked to the chemical make-up of biomass fuels. Combustion conditions are key. An important reason why biomass fuels have been observed to produce high levels of BrC is that they typically combust under relatively low-temperature fuel-rich conditions that are conducive for the formation of BrC [9,35]. On the other hand, fossil fuels, e.g. in internal combustion engines, are usually combusted at conditions (higher temperatures and more fuel-lean than biomass fuels) that are not conducive for BrC formation. As demonstrated by controlled-combustion experiments, the combustion conditions of benzene and toluene, both prevalent molecules in gasoline and diesel fuels, could be tuned to produce BrC with varying optical properties [10,14,25]. The same conclusion is inferred from a study that compared emissions from a compression-ignition engine operated using low-temperature combustion (LTC) strategies to conventional diesel combustion (CDC) [36,37]. When collected on quartz-fiber filters, particles from CDC had a black appearance, while particles from LTC had a brown appearance. This indicates that changing combustion strategy from CDC to LTC, while using the same fuel, could transform compression-ignition engines from BC producers to BrC producers.

Secondary reactions in the atmosphere are also significant sources of atmospheric BrC [16,17]. BrC has been observed in secondary organic aerosol (SOA) from the oxidation of aromatic VOC precursors, usually associated with combustion emissions [38–41]. Biogenic SOA is typically non-absorbing [39,42], though BrC was observed in biogenic SOA formed in the presence of ammonia

[43,44]. Secondary BrC also forms in the atmosphere via aqueous phase reactions of dicarbonyls [45–48], PAHs [49], and biomass-burning emissions [50]. Both gas-phase and heterogeneous reactions of PAHs with nitrate radicals produce secondary BrC or enhance primary-BrC absorption [23–25]. Furthermore, absorption by BrC chromophores can be enhanced by interactions with charge transfer complexes [51].

2.2. Optical-based classification of brown carbon

From the perspective of climate calculations, the importance of BrC stems from its ability to absorb solar radiation. Therefore, classifying BrC components based on their optical properties allows for practical implementation in models. The fundamental optical property is the complex refractive index ($m = n + ik$), where n is the real part, mostly linked to the scattering efficiency, and k is the imaginary part, mostly linked to the absorption efficiency [52]. For BrC, n is fairly constrained and wavelength independent in the visible spectrum, with reported values typically ranging between 1.5 and 1.7 [12,16,22,24,53]. On the other hand, BrC k values range over several orders of magnitude and can exhibit strong wavelength dependence in the visible spectrum [10,16,54]. The wavelength dependence of k is approximated with a power law, thus the wavelength-dependent k can be represented using 2 parameters: k at a specific wavelength (customarily chosen in the mid-visible, e.g. k at 550 nm, k_{550}) and the exponent of the power law (the wavelength dependence, w): $k(\lambda) = k_{550}\,[550/\lambda]^{w}$. Aerosol light absorption is often quantified using the mass absorption cross-section (MAC [m^2/g]), also referred to as the mass absorption efficiency (MAE). MAC depends on particle size and is not a true intensive property but it is a convenient property because it can be readily calculated from aerosol light-absorption and mass concentration measurements. The wavelength dependence of MAC, the absorption Ångström exponent (AAE) is related to w (AAE ≈ w + 1 in the small-particle limit).

k_{550} and w of different types of BrC compiled from 20 studies are plotted in Figure 1. Most of the studies did not report k_{550} and w directly, and some assumptions were made to convert the reported optical properties to k_{550} and w (see Supporting Information). Therefore, the values of the data points in Figure 1 are not meant to be accurate but are presented to convey general trends. It is informative to group the data as follows: 1) secondary BrC from aromatic VOCs [40,41,55,56]; 2) secondary BrC from biomass-combustion emissions [4,5]; 3) primary BrC from low-temperature pyrolysis / smoldering combustion of biomass fuels [22,35,54,57–60]; 4) primary BrC from high-temperature BC-producing biomass combustion [4,5,7,12,54,61]; and 5) low-volatility BrC, including BrC that survived high energy electron beam impact in a transmission electron microscope (TEM) [11] or heating to high temperatures in a thermodenuder [8,10,12].

There is a correlation between BrC absorption and its source. On average, the smallest k_{550} values are associated with secondary BrC from aromatic VOCs. BrC emitted from smoldering combustion exhibits approximately an order of magnitude increase in k_{550} over secondary BrC. BrC emitted from BC-producing combustion exhibits an additional order-of-magnitude increase in k_{550}, indicating a strong dependence of BrC absorption on combustion conditions [5,6,12] (Section 2.4). Low-volatility BrC exhibits another order-of-magnitude increase in absorption, with k_{550} values approaching that of BC. Secondary BrC formed from biomass-combustion emissions has k_{550} similar to primary biomass-combustion BrC, more than an order of magnitude larger than

secondary BrC from aromatic VOCs. This discrepancy warrants further investigation. One possible explanation is that the SOA precursors in biomass-combustion emissions likely include aromatic intermediate volatility organic compounds (IVOCs) and semi-volatile organic compounds (SVOCs) which produce SOA with more chromophoric functional groups than SOA from VOCs. Furthermore, the two studies that reported optical properties of secondary biomass-burning BrC featured only high-temperature BC-producing combustion [5,9]. There is a need for experiments that characterize secondary BrC from low-temperature smoldering biomass combustion.

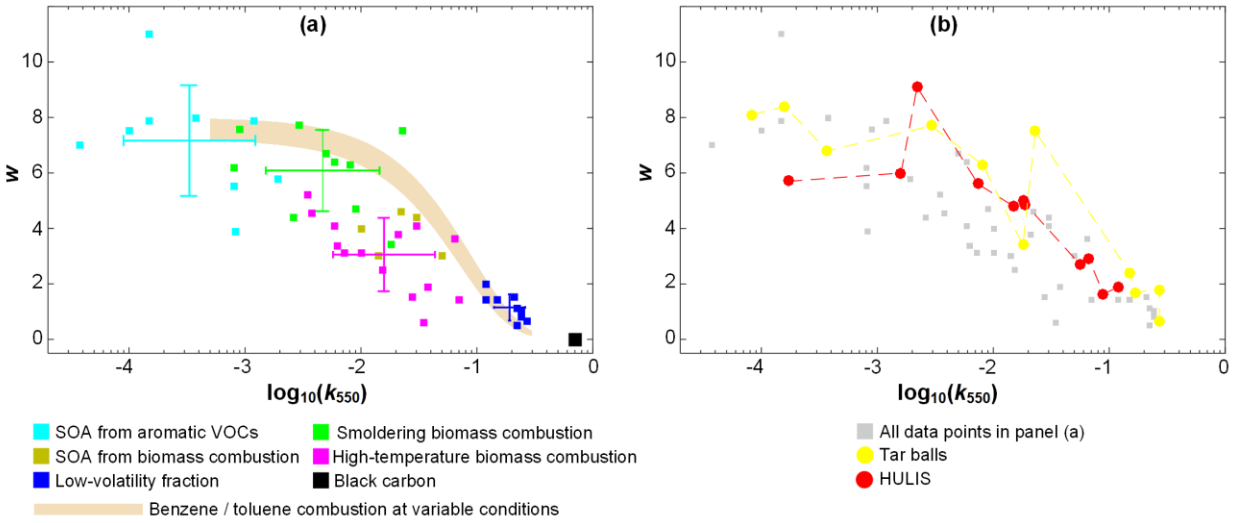

Figure 1. Compilation of BrC light-absorption properties obtained from various studies and represented in k_{550}-w space. Detailed information on the individual data points is given in Table S1 in the Supplementary Information. (a) Each symbol color (see legend) is associated with one of the five categories described in Section 2.2. The errorbars represent the mean and standard deviation (geometric for k_{550}) for each category. The shaded band represents the range of k_{550} vs w data obtained for BrC produced from controlled combustion of benzene and toluene [10]. Also shown are k_{550} and w of BC [62] for reference. (b) Compilation of tar balls (yellow) and HULIS (red) light-absorption properties obtained from various studies and represented in k_{550}-w space on top of the data points in panel (a) (grey). Detailed information on the individual data points is given in Table S1 in the Supplementary Information. Both tar balls and HULIS exhibit a large spread in k_{550} and w, similar to BrC in general.

k_{550} and w of BrC are highly variable and approach those of BC (Figure 1). Clearly, a robust representation of BrC in climate calculations requires a framework that accounts for this variability. For all BrC types/sources, k_{550} and w are inversely correlated, consistent with previous observations for specific types/sources including biomass-combustion [6,9,35,63], controlled combustion of benzene and toluene [10,14], as well as humic acids [64]. The w vs k_{550} relationship obtained for BrC from the controlled combustion of single-molecule fuels (benzene and toluene) [10] reproduces the general trend of w vs k_{550} of BrC from various primary and secondary sources, indicating a degree of universality of the w vs k_{550} relation. BrC can therefore be represented by a distribution along optical bins, each with a characteristic k_{550}-w pair. Guided by the distribution of data in Figure 1, a proposed optical-based classification of BrC is given in Figure 2 and Table 1. Due to the association between BrC light absorption and solubility (see below), this optical-based classification is in general consistent with the BrC classification of Corbin et al. [15] into soluble and insoluble (tar) BrC.

Table 1. Proposed brown optical-based carbon classes (Section 2.2).

BrC class	k_{550}	w	MAC_{550}* (m^2/g)	AAE*
Very weakly absorptive BrC **(VW-BrC)**	$10^{-4} – 10^{-3}$	6 – 9	$1.3x10^{-3} – 1.3 x10^{-2}$	7 – 10
Weakly absorptive BrC **(W-BrC)**	$10^{-3} – 10^{-2}$	4 – 7	$1.3x10^{-2} – 0.13$	5 – 8
Moderately absorptive BrC **(M-BrC)**	$10^{-2} – 10^{-1}$	1.5 – 4	0.13 – 1.3	2.5 – 5
Strongly absorptive BrC **(S-BrC)**	$> 10^{-1}$	0.5 – 1.5	> 1.3	1.5 – 2.5

*calculated from k_{550} and w using small-particle approximation (Supplementary Information) and assuming $n = 1.6$

BrC from a certain source is not uniform, but exhibits a distribution along the classes in Figure 2. For example, BrC from both smoldering and high-temperature combustion is expected to contain BrC from all the classes, but with different proportions: smoldering BrC is skewed more towards W-BrC and VW-BrC, while high-temperature BrC is skewed more towards M-BrC and S-BrC. To the first order, BrC sources can be mapped to classes: secondary BrC → VW-BrC, smoldering BrC → W-BrC, and high-temperature BrC → M-BrC. However, accurate representation of BrC in climate models, especially its evolution in the atmosphere (Section 3), requires the development of measurement techniques that could isolate each BrC class. This could be achieved by leveraging the associations between the light-absorption properties of BrC components and their physicochemical properties, including molecular size [10,15,65], volatility [6,9,10,15], and solubility [15,35,66,67]. BrC light absorption is inversely correlated with volatility. Therefore, optical distributions can be achieved by combining optical measurements with measurements of the mass fraction remaining (MFR) of BrC heated at different temperatures in a thermodenuder. Linking optical distributions with volatility distributions is appealing because it allows for efficient implementation in models [68] that employ a volatility basis set framework [69]. Optical distributions can also be achieved by sequential extraction of BrC in water and/or organic solvents. It should be noted, however, that the extraction efficiency of S-BrC is low both in water and organic solvents [15,67]. Therefore, measurements that rely on solvent extraction need to be coupled with airborne optical measurements to obtain the full BrC optical distribution. S-BrC is of special interest not only because of its strong absorption, but also because of its potential resistance to loss in the atmosphere (Section 3). The S-BrC class was constructed based on previous reports (Figure 1, Table S1) that utilized different terminologies including: brown carbon spheres [11], extremely low volatility organic compounds (ELVOCs) [9], refractory BrC [10], intermediate absorber (i.e. between BrC and BC) [8], and tar BrC [15].

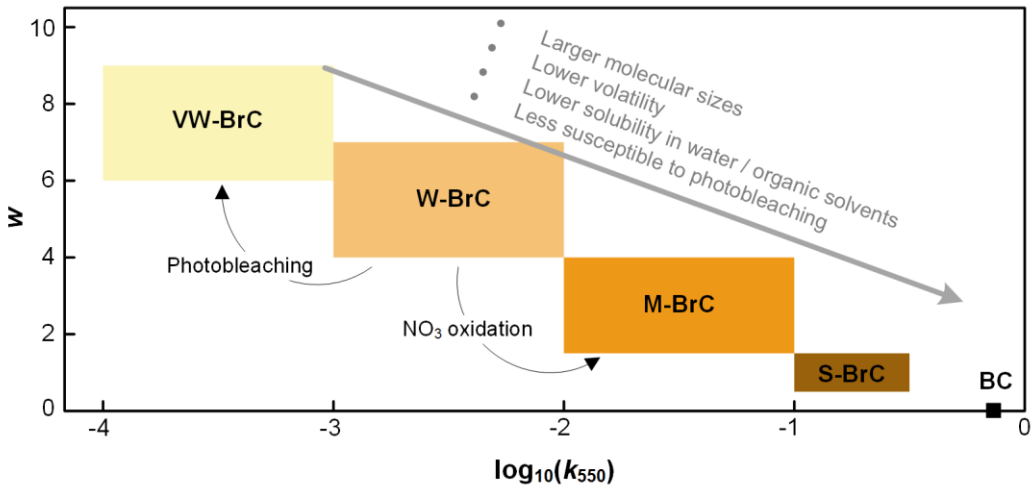

Figure 2. Graphical representation of the optical-based BrC classes in k_{550}-w space (Section 2.2). Also shown is BC [62] for references. The continuum of optical properties characterizing the classes is expected to be associated with a continuum of physicochemical properties, including molecular sizes, volatility, and solubility. This association can be exploited to design experiments that retrieve BrC optical distributions from measurements. Utilizing this framework to represent BrC in climate models enables accounting for variability in BrC absorption as well as the decay / enhancement of BrC absorption upon atmospheric aging (Section 3).

2.3. HULIS and tar balls

HULIS and tar balls have been extensively studied as components of BrC [17,28]. HULIS are mostly associated with chemically processed biomass-combustion smoke and SOA from biogenic and anthropogenic precursors [17], but have also been observed in fresh biomass-combustion emissions [31]. "Tar balls" were introduced by Pósfai et al. [70] to designate biomass-combustion carbonaceous particles that are spherical and stable under the electron beam and high vacuum of a TEM. Similar characteristics are still used to identify tar balls [71–74], however, there is a disagreement on their formation pathways. Some studies proposed a mechanism that involves high-temperature transformation of wood tar [74–76], while other studies asserted that heterogeneous chemical processing is required to transform biomass-combustion particles into tar balls [72,73].

While measurements performed under the umbrellas of HULIS and tar balls have provided valuable contributions to the understanding of BrC, they have also revealed highly variable and overlapping physicochemical and optical properties between the two categories. Laskin et al. [17] pointed out the similarities in chemical characteristics of HULIS and tar balls (similar degrees of sp^2 hybridization and oxygenation). Prominent BrC chemical constituents (e.g. nitrated aromatics) were identified in both HULIS [31,77] and tar balls [53]. k_{550} and w compiled from various studies on HULIS [64,78–80] and tar balls [11,24,58,60,75] are plotted in Figure 1b. Neither HULIS nor tar balls exhibit uniform optical properties but rather the same level of variability as BrC in general. For the purpose of efficient representation in models, HULIS and tar balls can be conveniently absorbed into the optical-based classes proposed in Section 2.2.

There is a disconnect between a key characteristic in the operational definition of tar balls (survival in the TEM) and the fact that their reported optical properties are often obtained from

measurements of airborne particles. It is almost certain that the airborne particles include constituents that would be lost by volatilization in the TEM [70]. The constituents that volatilize are less absorbing than the constituents that survive in the TEM. In fact, k_{550} of tar balls obtained for airborne particles [24,58,60] (with the exception of Hoffer et al. [75]) are 1-2 orders of magnitude smaller than k_{550} of particles that survived in the TEM [11] (Table S1). It is noteworthy that unlike other studies, the tar balls in Hoffer et al. [75] were generated under controlled conditions where they were subjected to thermal shock at a uniform temperature. It is likely that the conditions in that study produced highly absorptive tar balls with relatively uniform properties. If we consider the strict definition of tar balls (survive in the TEM), it follows that they have extremely low volatilities and are strongly absorptive, and thus belong to S-BrC (Figure 2).

2.4. The BC-to-OA ratio as a basis for brown-carbon parameterizations

Emission factors and physicochemical properties of gaseous and particulate emissions from combustion largely depend on combustion conditions (temperature and equivalence ratio). In the uncontrolled combustion of biomass, quantifying the temperature and equivalence ratio is not possible. Combustion conditions are obtained indirectly using the modified combustion efficiency (MCE) [81], defined as the relative amount of CO_2 to CO_2 + CO emitted from combustion. Therefore, it is expected that the properties of combustion aerosol (BC and BrC), including optical properties, can be parameterized as a function of MCE. However, several studied reported that robust correlations of optical properties with MCE could not be obtained [6,82,83].

Saleh et al. [9] showed that k_{550} and w of BrC emitted from biomass combustion were well correlated with another proxy of combustion conditions, namely the BC-to-OA ratio (BC/OA). Specifically, BrC becomes darker (k_{550} increases and w decreases) with increasing BC/OA. The dependence of BrC absorption on BC/OA was confirmed in laboratory studies of biomass [5,6] and biofuel [7] combustion, field observations [32], as well as in comparing climate-model output with satellite observations [84]. The fundamental reasoning behind the increase in BrC absorption with increasing BC/OA is that a fraction of BrC is comprised of organic precursors of BC (mostly PAHs) whose conversion to BC was not complete in the combustion process. The optical properties of the precursors converge towards those of BC as they approach the BC-formation threshold [10]. These precursors are referred to as incipient soot in the combustion literature, as opposed to mature soot whose definition is more closely related to BC [85–87]. Uncontrolled biomass combustion features a wide range of combustion conditions [81], thus a wide distribution along BrC classes. When the combustion conditions are conducive for BC formation (high BC/OA), the BrC distribution is skewed towards BC precursors that are close to the BC-formation threshold (S-BrC). For combustion conditions that are not conducive for BC formation (low BC/OA), the BrC distribution is skewed towards less mature precursors (W-BrC). This explains the difference in BrC k_{550} and w between smoldering and BC-producing biomass combustion in Figure 1a.

Figure 3 shows three parameterizations of BrC k_{550} and w as a function of BC/OA obtained from laboratory biomass-combustion experiments [6,9] and analysis of data from several biomass- and biofuel-combustion experiments and field observations [63]. The three parameterizations show

qualitatively similar trends, albeit with significant differences in the values of k_{550} and w at each BC/OA. These differences largely reflect biases associated with challenges in retrieving BrC light-absorption properties from online measurements and differences in employed techniques (Section 2.5). There is no clear case to be made for one parameterization over the others for BC/OA > 0.005. It should be noted that the data of Saleh et al. [9] constituted a substantial fraction of the data used in the fit of Lu et al. [63], thus the closer agreement between the two. For BC/OA < 0.005, the parameterization of Saleh et al. [9] could yield unphysical results (negative k_{550}) because that involves extrapolating the fit beyond the limits of the experimental data in that study. The parameterizations of McClure et al. [6] and Lu et al. [63] are more appropriate for smoldering conditions (i.e. with very low BC/OA). It should be noted, however, that current emission inventories [81,88] employed in modeling frameworks are constructed based on average emissions for fuel / land-cover classes, and thus do not account for the low (smoldering) and high (highly flaming) extremes in BC/OA. Typically, the range of BC/OA in emission inventories is ~10^{-2} – 10^{-1}.

Measurements that produce BC/OA parameterizations could be readily expanded to retrieve BrC optical distributions by incorporating thermodenuder measurements and/or sequential solvent extraction. McClure et al. [6] performed thermodenuder measurements at 300 °C and found that the OA MFR increased with increasing BC/OA, indicating an increased abundance of low-volatility components, consistent with the established association between BrC light-absorption properties and volatility (Section 2.2). Light-absorption properties of the residual BrC were not reported, but given the high thermodenuder temperature, the residual BrC is expected to be S-BrC.

Retrieving BrC optical properties from combustion emissions that contain BC and BrC requires the challenging task of decoupling their absorption. A simplified practical approach involves parameterizing the effective optical properties (e.g. MAC, AAE, single scattering albedo (SSA)) of the mixed BC + BrC (or OA) aerosol as a function of BC/OA [14,67,82]. Parameterizations obtained from this approach also exhibit increase in absorption with increasing BC/OA due to both an increase in BrC absorption and BC mass fraction.

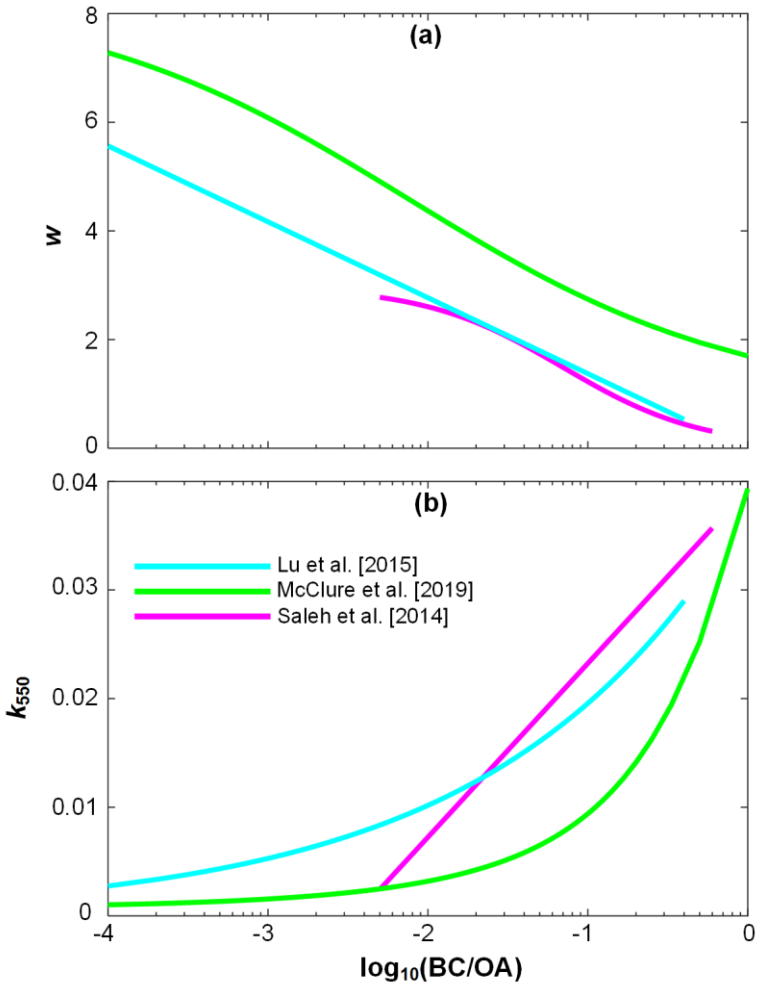

Figure 3. Parameterizations of biomass-combustion BrC (a) w and (b) k_{550} as a function of BC/OA. The corresponding equations can be found in the respective studies (Lu et al. [63], McClure et al. [6], and Saleh et al. [9]) and in the Supplementary Information.

2.5. Measurement challenges, biases, and needs

Informative reviews of the techniques employed for speciating BrC and measuring its optical properties can be found in Laskin et al. [17] and Moise et al. [16]. This sub-section focuses on some of the challenges associated with current measurement techniques and the biases induced when attempting to translate measurements into parameters used in climate models.

Many of the BrC measurements have either missed S-BrC or attributed its absorption to BC [8,10,67]. As pointed out by Hoffer et al. [13], apportioning absorption between BC and BrC is often based on the assumption that only BC absorbs in the red wavelengths, leading to S-BrC being partially misapportioned to BC. Due to its low solubility or insolubility in water and organic solvents [15,67], solvent-extraction methods largely miss S-BrC.

The varying levels of solubility of BrC classes in different solvents can be exploited to obtain BrC optical distributions. Shetty et al. [67] extracted biomass-combustion BrC using water, methanol, and acetone. They found that the extraction efficiency was highest for acetone and lowest for

water. They also reported that the extraction efficiency for all solvents decreased with increasing BC/OA, consistent with increased production of S-BrC at high BC/OA. Combining bulk optical measurements after sequential extraction in water, methanol, and acetone (or other solvents) with online measurements can yield information on the relative abundance of the different BrC classes, including S-BrC.

Retrieved BrC optical properties from online measurements are subject to biases associated with measurement techniques and choice of instrument calibration standards. Photoacoustic instruments are widely accepted to provide accurate absorption measurements, while filter-based instruments have the advantage of being robust and less expensive [89]. Comparisons between the two techniques have shown that filter-based measurements overestimate absorption, but the wavelength dependence (AAE) from the two techniques are in relatively better agreement [9,89,90]. Correction algorithms, including a recently developed "universal" algorithm ([89] and references within), can be used to better interpret filter-based measurements. For photoacoustic measurements, the measured absorption depends on the choice of calibration method [91]. Currently employed calibration standards include gaseous (O_3, NO_2) and particulate (e.g. nigrosin) absorbers [90–93]. A universal calibration standard/approach is necessary for better interpretation of data obtained from different studies.

BrC and BC often exist in the same population, making it challenging to isolate and characterize the BrC optical properties. This can be done numerically via optical closure, but the retrieved BrC properties are sensitive to the assumed mixing state and morphology of BC in the optical calculations [94]. For biomass-combustion emissions, especially at low BC/OA, most of the BrC is externally mixed with BC [6]. Adler et al. [8] relied on the difference in morphology between externally mixed BrC particles and BC-containing particles and employed sequential electrical-mobility (using a differential mobility analyzer, DMA) and mass selection (using a centrifugal particle mass analyzer, CPMA) to isolate and characterize BrC particles. For a comprehensive discussion of challenges associated with characterizing mixing state and morphology, readers are referred to the recent review by Stevens and Ashu [95].

3. Evolution of brown carbon in the atmosphere

3.1. Photobleaching (daytime aging)

Atmospheric aging influences BrC light-absorption properties. The most well-studied phenomenon is the photo-initiated loss of chromophores (photobleaching) of secondary BrC in the aqueous phase [19,44,96–98]. Those studies reported rapid photobleaching, on the order of minutes to hours, suggesting that the lifetime of secondary-BrC absorption could be much shorter than the supposed lifetime of the aerosol (days). Photobleaching was also observed for smoldering biomass-combustion BrC in the aqueous phase [19,96] and the aerosol phase [21,22], but with three key differences from secondary BrC: 1) combustion BrC exhibits a period photoenhancement prior to photobleaching [19,20,96]; 2) the decay of absorption occurs at longer timescales than secondary BrC [19]; and 3) a fraction of combustion BrC is resistant to photobleaching. Browne et al. [22] and Sumlin et al. [21] reported that the near-UV k of BrC from smoldering biomass combustion retained ~60%-70% of its original value after multiple-day

equivalent photo-oxidation in an oxidation flow reactor (OFR). Using size exclusion chromatography (SEC), Wong et al. [96] investigated photo-initiated aging (OH oxidation and UV photolysis) in the aqueous phase of smoldering biomass-combustion BrC segregated by molecular size. OH oxidation was the dominant mechanism for bleaching of molecules < 400 Da, while photolysis was the dominant mechanism for molecules > 400 Da. Absorption decay of the large molecules was much slower, indicating that the large BrC molecules are more persistent in the atmosphere. Atmospheric observations of the evolution of biomass-combustion BrC paint a qualitatively similar picture to laboratory measurements [18,32,96]: BrC absorption decays, but the decay eventually levels out. However, atmospheric observations have reported longer BrC-absorption lifetimes (~1 day) than laboratory experiments (hours).

The studies discussed above largely miss S-BrC (Figure 2). Molecular-size-segregated measurements of the water- and methanol-soluble BrC [96] show that the larger soluble molecules were more resistant to photobleaching. This suggests that the even larger insoluble S-BrC molecules would be even more resistant. All the laboratory studies focused on smoldering/pyrolysis BrC, whose optical distribution is skewed toward the small-molecular-size W-BrC relative to BrC produced in high-temperature combustion (Figure 1). Therefore, smoldering BrC is expected to be more susceptible to photobleaching than high-temperature BrC. This could partly explain the difference in observed BrC lifetime between laboratory measurements and field observations, where the BrC could come from both smoldering and high-temperature biomass combustion. Experiments that investigate photobleaching of high-temperature biomass-combustion BrC as well as isolate S-BrC are needed to fill this gap.

3.2. Enhancement in absorption due to reactions with NO_3 (nighttime aging)

Photobleaching of BrC was shown to slow down [20] or halt [53] at high NOx conditions due to the formation of nitrogen-containing chromophores. Nitrogen-containing chromophores also form due to reactions with NO_3 radicals. For example, PAHs, important constituents of combustion emissions, undergo gas-phase and heterogeneous oxidation with NO_3 to produce nitro-PAHs [99] that are less volatile and more light-absorbing than their parent PAHs. At nighttime, the high production rate of NO_3 makes the heterogeneous oxidation with BrC and the consequent enhancement of its absorption important at atmospheric conditions [24]. Observations of the nighttime evolution of biomass-combustion emissions are scarce. One study reported that in the night hours following a bonfire event, aged biomass-combustion BrC was enriched with nitroaromatic species that were hypothesized to have formed via NO_3 oxidation of primary BrC [23]. Furthermore, BrC light absorption was significantly enhanced after several hours of nighttime aging [100]. The importance of heterogeneous NO_3 oxidation in enhancing BrC absorption was recently confirmed in the laboratory, where after 13.3 hours of equivalent atmospheric NO_3 aging in an OFR, k of BrC produced from wood tar increased by more than a factor of 2 in the visible and 40% in the UV wavelengths [24]. In another laboratory study, 2 nights of equivalent atmospheric NO_3-induced heterogeneous oxidation in an OFR led to ~50% increase in mid-visible k of BrC produced from toluene combustion [25]. More laboratory experiments and observations of nighttime evolution of biomass-burning plumes are needed to further elucidate the effects of NO_3 aging.

4. Brown carbon in climate models

There has been a growing number of attempts to represent BrC absorption in column [26], regional [101,102], and global [84,103–110] climate calculations. Table 2 provides a summary of the global-scale studies that accounted for BrC absorption. The direct radiative effect (DRE) in Table 2 is defined as the difference in net radiative flux with and without BrC absorption, which is different from the conventional aerosol DRE defined as the difference in net radiative flux with and without the aerosol. Following Wang et al. [110], "BrC absorption DRE" is used to stress this distinction. The reported global-mean BrC absorption DRE values range between +0.03 W/m^2 and +0.57 W/m^2. BrC absorption DRE is localized over regions with high biomass-burning activity (South America, Africa, Southeast Asia) where it reaches values larger than +1 W/m^2 [103,104,106,107,110], significantly larger than the global-average DRE (Table 2).

The subsequent sub-sections discuss the current treatments of BrC in climate models, sources of uncertainty that lead to the large range in BrC absorption DRE, and potential improvements to achieve better accuracy in predicting BrC absorption DRE. The sources of uncertainty addressed here are only those pertaining specifically to BrC. There are numerous challenges associated with modeling aerosol climate effects in general (e.g. radiative transfer schemes, cloud parameterizations, deposition mechanisms, etc.) that are not addressed in this review. Furthermore, there are important radiative effects of BrC absorption besides DRE that are not discussed here, including the semidirect effect [108], other cloud absorption effects [105], and BrC deposition on snow [28,66].

4.1. Brown carbon sources and light-absorption properties

Supported by experimental and observational data, there is a consensus that OA from biomass and biofuel combustion should be treated as BrC in climate models. As described below, this can be conveniently implemented using a BC/OA-type parameterization. OA from fossil-fuel combustion, on the other hand, is assumed to be non-absorbing. This is justified because fossil fuels are usually combusted at conditions that are not conducive for BrC formation (Section 2.1). There are two major exceptions: low-efficiency residential-coal combustion [27,28,33] and HFO in ship engines [15,34]. Both these BrC sources are not accounted for in current models. Secondary BrC from aromatic VOCs was incorporated in some climate-modeling studies [107,109,110]. As shown in Figure 1, k_{550} of secondary BrC is 1-2 orders of magnitude smaller than combustion BrC and therefore has a smaller contribution to BrC absorption DRE. However, k of secondary BrC has a steep wavelength dependence and it can potentially have an important effect on photochemistry due to its UV absorption [84,107].

A challenge associated with representing BrC absorption in climate models is the large variability in reported BrC light-absorption properties. As described in Section 2.2, this is a manifestation of the diversity in BrC classes and is not a mere consequence of measurement uncertainties (though such uncertainties do exist, Section 2.5). Feng et al. [103] and Lin et al. [104] investigated the sensitivity of BrC absorption DRE to assumed BrC k by performing calculations either with weakly or moderately absorbing BrC. The difference in assumed k induced a discrepancy of more than a factor of 2 in BrC absorption DRE, indicating that accurate representation of BrC in climate calculations requires an explicit account of its variability.

Saleh et al. [9] showed that the variability in k of BrC in biomass-combustion emissions largely depends on combustion conditions and can be parameterized as a function of BC/OA (Section 2.4). Since BC/OA is readily inferred from emission inventories [81,111], this parameterization enables representing spatial variability in k of BrC emissions. The importance of accounting for spatial variability in k was demonstrated by Hammer et al. [84] who showed that in order to match modeled and observed UVAI, larger BrC k values were required over regions dominated by grassland fires (Africa) than regions dominated by forest fires (South America). Typically, grassland fires have larger BC/OA than forest fires [81], thus this finding is consistent with the established BrC k dependence on BC/OA [5,6,9,63].

As described in Section 2.2, the representation of BrC absorption in climate models can be potentially improved by distributing BrC into optical bins (e.g. Figure 2), which is especially important for representing BrC aging (Section 4.3). This approach was somewhat employed in studies that differentiated between biomass/biofuel BrC and secondary BrC [107,109,110] and a study that split biomass/biofuel BrC into tar balls (analogous to S-BrC in Figure 2) and BrC (analogous to M-BrC in Figure 2) [105].

4.2. Black carbon or brown carbon? Emission inventories and field measurements

Emission rates of BC and OA from biomass combustion are usually estimated by combining fuel-burn data obtained from remote-sensing platforms (e.g. MODIS) with emission factors compiled from laboratory and field measurements [111,112]. This procedure is extremely challenging both on the remote-sensing [111] and emission-factor [81] sides. A detailed discussion of emission inventories is beyond the scope of this review. Here, I focus on one issue that directly affects BrC (and BC) representation in models.

The most up-to-date emission inventories of biomass and biofuel combustion (e.g. GFED4 [112] and FINN [111]) rely on emission factors of BC and OA obtained primarily from thermal-optical measurements (Akagi et al. [81] and references within) that report EC and OC. An implicit assumption in climate models is that BC is equivalent to EC. While this assumption is justified to a certain extent for combustion sources that do not emit substantial amounts of BrC (e.g. diesel engines), it induces bias for biomass and biofuel combustion. The thermal-optical technique relies on the assumption that OC is non-absorbing in the visible spectrum (e.g. at 633 nm in the Sunset OCEC analyzer). The presence of BrC, especially S-BrC, leads to the instrument reporting "artificial" EC [14]. By performing controlled-combustion experiments, Cheng et al. [14] showed that EC/OC ≈ 0.4 was reported by an OCEC analyzer for S-BrC, indicating that a substantial fraction of S-BrC can be counted as EC in emission inventories, therefore as BC is climate models.

To illustrate the potential importance of this bias, assume that EC/OC of S-BrC is 0.4 [14] (i.e. ~30% of S-BrC is counted as BC) and that S-BrC constitutes ~10% of biomass-combustion OA [9]. The global-average BC/OA of biomass and biofuel combustion are 0.05 and 0.12, respectively [110]. Therefore, ~60% of biomass BC and ~25% of biofuel BC in climate models could be S-BrC misattributed to BC. While this is a simplified calculation, it suggests that misattribution of S-BrC to BC severely biases the BC and BrC budgets in climate models and should be further investigated. A case could be made that lumping S-BrC with BC might be practical given the similarity in their optical properties (Figure 3). However, caution should be practiced when

constraining models using field/aircraft observations. For example, when using BC observations obtained using a single-particle soot photometer (SP2) to constrain model output [110], it should be noted that the modeled and observed BC are not equivalent: modeled BC is EC and is biased high due to the S-BrC contribution to EC. Therefore, adjusting the modeled BC to match observations would lead to underestimation of BC (and BrC) concentrations.

Recent laboratory studies and field/aircraft campaigns have increasingly relied on state-of-the-art techniques to quantify BC (e.g. SP2) [6,9,113,114] and BrC (e.g. optical closure by combining measurements from complimentary online instruments [5,6,9], online solvent extraction [18,26]). Therefore, it is expected that next-generation emission inventories will make use of these improved measurements, which promises to improve the accuracy of BC and BrC representation in climate models. Ideally, emission inventories will include BrC as a sub-category of OA with BrC being split into several optical bins (e.g. Figure 2).

4.3. Atmospheric aging

As described in Section 3, the light-absorption properties of BrC evolve upon atmospheric aging. Wang et al. [110] was the first study to incorporate a BrC photobleaching scheme in a climate-modeling framework. They assumed that BrC absorption decreased following a first-order dynamic response with a time constant $\tau = \frac{5\times10^5}{[OH]}$, ([OH], molecules/cm^3) chosen to be consistent with observed BrC absorption lifetimes of ~1 day [18,32]. They found that BrC absorption DRE dropped from +0.1 W/m^2 to + 0.048 W/m^2 when accounting for BrC photobleaching. Brown et al. [108] reported similar results (BrC absorption DRE dropped from +0.13 W/m^2 to + 0.06 W/m^2) when they incorporated the same BrC photobleaching scheme. Wang et al. [110] reported that accounting for BrC photobleaching resulted in better agreement with BrC absorption measured in two aircraft campaigns [114] and concluded that neglecting BrC photobleaching results in an overestimation of BrC absorption DRE. However, BrC absorption in these campaigns was obtained by solvent extraction (water and methanol), which would substantially underestimate total BrC absorption because a fraction of BrC, especially S-BrC, is insoluble [15,67] (Section 2.5). Therefore, it is likely that the photobleaching scheme employed by Wang et al. [110] and Brown et al. [108] results in an underestimation in BrC absorption DRE.

The attempts [108,110] to represent BrC aging is a promising first step. However, as pointed out by Wang et al. [110], observational data on the atmospheric evolution of BrC are scarce, and more measurements are needed to better constrain the models. Furthermore, as described in Section 3.2, there is emerging evidence that nighttime darkening of BrC due to NO_3 oxidation can be important. Campaigns that track the nighttime evolution of biomass-combustion plumes are needed in order to provide the data required to represent nighttime BrC darkening in models.

As described in Section 3, the large-molecular-size BrC is less susceptible to photobleaching than the small-molecular size BrC [96]. Improved representation of photobleaching can be achieved by distributing BrC into several optical bins (e.g. Figure 2) and dynamically moving BrC from the more-absorptive bins to the less-absorptive bins as a function of atmospheric age. The same binning scheme can be utilized to represent NO_3-induced darkening.

5. Conclusions

Compiling BrC light-absorption measurements reported in 20 studies revealed a continuum of BrC light-absorption properties with k_{550} ranging between ~10^{-4} and ~10^{-1} and w ranging between ~10 and ~1. Accounting for this variability is necessary for accurate representation of BrC in climate calculations. BrC was grouped in four classes, each with characteristic k_{550}-w: very weakly absorbing (VW-BrC), weakly absorbing (W-BrC), moderately absorbing (M-BrC), and strongly absorbing (S-BrC). This approach can be utilized to develop parameterizations that distribute BrC from various sources into optical bins by exploiting correlations between BrC light absorption and its molecular size, volatility, and solubility in water and organic solvents. To the first order, BrC classes can be mapped to sources: VW-BrC → secondary BrC, W-BrC → BrC from smoldering-combustion, and M-BrC → BrC from BC-producing combustion.

Photobleaching of BrC chromophores upon atmospheric aging is an important phenomenon that should be accounted for in climate calculations. There is evidence that susceptibility to photobleaching decreases with increasing molecular size (correlated with absorption), which can potentially be represented using the optical-binning approach. New evidence indicates that nighttime heterogeneous oxidation with NO_3 enhances BrC absorption. More experiments and field observations are needed to quantify this effect.

S-BrC has optical properties close to those of BC and is especially important to account for in climate calculations. S-BrC has been largely missed in measurements that relied on solvent extraction or misattributed to BC in measurements that assumed no BrC absorption in the long-visible wavelengths. Furthermore, a substantial fraction of S-BrC is reported as EC in thermal-optical measurements on which emission inventories primarily rely. Since BC in atmospheric/climate models is equivalent to EC from emission inventories, a significant fraction of BC in models is potentially S-BrC misattributed to BC. Caution should be practiced when utilizing BC observations that are not sensitive to S-BrC (e.g. SP2) to constrain BC model output.

Climate models that represent BrC absorption account for BrC emissions from biomass and biofuel combustion and some account for secondary BrC from aromatic VOCs. Recent observations indicate that low-efficiency coal combustion and ship engines utilizing HFO are important BrC sources that should also be accounted for in models.

Acknowledgments

I would like to thank Dr. Yele Sun and Dr. Hongliang Zhang for the invitation to contribute this article. Financial support was provided by the National Science Foundation, Division of Atmospheric and Geospace Sciences (AGS- 1748080).

Table 2. Summary of BrC treatments in global climate models

Study	BrC sources	BrC optical properties	Mixing state / morphology	Photo-bleaching	Aerosol-cloud interactions	BrC absorption DRE (W/m²)
Feng et al. 2013 [103]	66% of biomass/biofuel OA	Weakly absorbing BrC: [35] Moderately absorbing BrC: [61]	Internally mixed core-shell	No	No	+0.04 (weakly absorbing BrC) +0.11 (moderately absorbing BrC)
Jacobson 2014 [105]	30% of biomass/biofuel OA are tar balls; the rest are moderately absorbing BrC	Tar balls: [11] Moderately absorbing BrC: [61]	Internally mixed core-shell	No	Yes	N/A
Lin et al. 2014 [104]	Biomass/biofuel OA and biogenic/anthropogenic SOA	Weakly absorbing BrC: [35] Moderately absorbing BrC: [61]	Externally mixed	No	No	+0.22 (weakly absorbing BrC) +0.57 (moderately absorbing BrC)
Wang et al. 2014 [109]	25% of biomass OA, 50% of biofuel POA, aromatic SOA	Average of [35,115,116]	Externally mixed with constant BC lensing factor (1.1 for fossil fuel BC and 1.5 for biomass/biofuel BC)	No	No	+0.07
Saleh et al. 2015 [106]	Biomass/biofuel OA	BC/OA parameterization [9]	Internally mixed core-shell; Externally mixed	No	No	+0.12 (internally mixed core-shell) +0.22 (externally mixed)
Jo et al. 2016 [107]	Biomass/biofuel OA; aromatic SOA	biomass/biofuel OA: [117] aromatic SOA: [118]	Externally mixed	No	No	+0.11
Hammer et al. 2016 [84]	Biomass OA	Constrained by OMI UVAI	Externally mixed	No	No	+0.03
Wang et al. 2018 [110]	Biomass/biofuel OA; aromatic SOA	biomass/biofuel OA: BC/OA parameterization [9] aromatic SOA: [115]	Externally mixed with constant BC lensing factor (1.1 for fossil fuel BC and 1.5 for biomass/biofuel BC)	Yes	No	+0.048 (with photobleaching) +0.1 (no photobleaching)
Brown et al. 2018 [108]	Biomass/biofuel OA	BC/OA parameterization [9]	Internally mixed with volume mixing	Yes	Yes	+0.06 (with photobleaching) +0.13 (no photobleaching)

Conflict of interest statement

There is no conflict of interest.

References

1. Patterson EM, McMahon CK. Absorption characteristics of forest fire particulate matter. Atmos Environ. 1984;18:2541–51.

2. Mukai H, Ambe Y. Characterization of a humic acid-like brown substance in airborne particulate matter and tentative identification of its origin. Atmos Environ. 1986;20:813–9.

3. Andreae MO, Gelencser A. Black carbon or brown carbon? The nature of light-absorbing carbonaceous aerosols. Atmos Chem Phys. 2006;6:3131–48.

4. Saleh R, Hennigan CJ, McMeeking GR, Chuang WK, Robinson ES, Coe H, et al. Absorptivity of brown carbon in fresh and photo-chemically aged biomass-burning emissions. Atmos Chem Phys. 2013;13.

5. Kumar NK, Corbin JC, Bruns EA, Massabó D, Slowik JG, Drinovec L, et al. Production of particulate brown carbon during atmospheric aging of residential wood-burning emissions. Atmos Chem Phys [Internet]. 2018;18:17843–61. Available from: https://www.atmos-chem-phys.net/18/17843/2018/

6. McClure CD, Lim CY, Hagan DH, Kroll JH, Cappa CD. Biomass-burning derived particles from a wide variety of fuels: Part 1: Properties of primary particles. Atmos Chem Phys Discuss [Internet]. 2019;2019:1–37. Available from: https://www.atmos-chem-phys-discuss.net/acp-2019-707/

7. Xie M, Shen G, Holder AL, Hays MD, Jetter JJ. Light absorption of organic carbon emitted from burning wood, charcoal, and kerosene in household cookstoves. Environ Pollut [Internet]. 2018;240:60–7. Available from: http://www.sciencedirect.com/science/article/pii/S0269749118303476

8. Adler G, Wagner NL, Lamb KD, Manfred KM, Schwarz JP, Franchin A, et al. Evidence in biomass burning smoke for a light-absorbing aerosol with properties intermediate between brown and black carbon. Aerosol Sci Technol [Internet]. Taylor & Francis; 2019;53:976–89. Available from: https://doi.org/10.1080/02786826.2019.1617832

9. Saleh R, Robinson ES, Tkacik DS, Ahern AT, Liu S, Aiken AC, et al. Brownness of organics in aerosols from biomass burning linked to their black carbon content. Nat Geosci. 2014;DOI: 10.1038/NGEO2220.

10. Saleh R, Cheng Z, Atwi K. The Brown–Black Continuum of Light-Absorbing Combustion Aerosols. Environ Sci Technol Lett [Internet]. American Chemical Society; 2018;5:508–13. Available from: https://doi.org/10.1021/acs.estlett.8b00305

11. Alexander DTL, Crozier P a, Anderson JR. Brown carbon spheres in East Asian outflow and their optical properties. Science [Internet]. 2008 [cited 2012 Oct 30];321:833–6. Available from: http://www.ncbi.nlm.nih.gov/pubmed/18687964

12. Saleh R, Robinson ES, Tkacik DS, Ahern AT, Liu S, Aiken AC, et al. Brownness of organics in aerosols from biomass burning linked to their black carbon content. Nat Geosci. 2014;7.

13. Hoffer A, Tóth Á, Pósfai M, Chung CE, Gelencsér A. Brown carbon absorption in the red and near-infrared spectral region. Atmos Meas Tech. 2017;10:2353–9.

14. Cheng Z, Atwi K, Onyima T, Saleh R. Investigating the dependence of light-absorption properties of combustion carbonaceous aerosols on combustion conditions. Aerosol Sci Technol [Internet]. Taylor & Francis; 2019;1–16. Available from: https://doi.org/10.1080/02786826.2019.1566593

15. Corbin JC, Czech H, Massabò D, de Mongeot FB, Jakobi G, Liu F, et al. Infrared-absorbing carbonaceous tar can dominate light absorption by marine-engine exhaust. npj Clim Atmos Sci [Internet]. 2019;2:12. Available from: https://doi.org/10.1038/s41612-019-0069-5

16. Moise T, Flores JM, Rudich Y. Optical Properties of Secondary Organic Aerosols and Their Changes by Chemical Processes. Chem Rev. 2015;115:4400–39.

17. Laskin A, Laskin J, Nizkorodov S a. Chemistry of Atmospheric Brown Carbon. Chem Rev [Internet]. 2015;DOI: 10.1021/cr5006167. Available from: http://pubs.acs.org/doi/abs/10.1021/cr5006167

18. Forrister H, Liu J, Scheuer E, Dibb J, Ziemba L, Thornhill KL, et al. Evolution of brown carbon in wildfire plumes. Geophys Res Lett. 2015;42:4623–30.

19. Wong JPS, Nenes A, Weber RJ. Changes in Light Absorptivity of Molecular Weight Separated Brown Carbon Due to Photolytic Aging. Environ Sci Technol [Internet]. American Chemical Society; 2017;51:8414–21. Available from: https://doi.org/10.1021/acs.est.7b01739

20. Zhong M, Jang M. Dynamic light absorption of biomass-burning organic carbon photochemically aged under natural sunlight. Atmos Chem Phys. 2014;14:1517–25.

21. Sumlin BJ, Pandey A, Walker MJ, Pattison RS, Williams BJ, Chakrabarty RK. Atmospheric Photooxidation Diminishes Light Absorption by Primary Brown Carbon Aerosol from Biomass Burning. Environ Sci Technol Lett [Internet]. American Chemical Society; 2017;4:540–5. Available from: https://doi.org/10.1021/acs.estlett.7b00393

22. Browne EC, Zhang X, Franklin JP, Ridley KJ, Kirchstetter TW, Wilson KR, et al. Effect of heterogeneous oxidative aging on light absorption by biomass burning organic aerosol. Aerosol Sci Technol [Internet]. Taylor & Francis; 2019;53:663–74. Available from: https://doi.org/10.1080/02786826.2019.1599321

23. Lin P, Bluvshtein N, Rudich Y, Nizkorodov SA, Laskin J, Laskin A. Molecular Chemistry of Atmospheric Brown Carbon Inferred from a Nationwide Biomass Burning Event. Environ Sci Technol. 2017;51:11561–70.

24. Li C, He Q, Hettiyadura APS, Käfer U, Shmul G, Meidan D, et al. Formation of Secondary Brown Carbon in Biomass Burning Aerosol Proxies through NO3 Radical Reactions. Environ Sci Technol [Internet]. American Chemical Society; 2019; Available from: https://doi.org/10.1021/acs.est.9b05641

25. Cheng Z, Atwi KM, Yu Z, Avery A, Fortner EC, Williams L, et al. Evolution of the Light-absorption Properties of Combustion Brown Carbon Aerosols Following Reaction with Nitrate Radicals. Aerosol Sci Technol [Internet]. Taylor & Francis; 2020;1–18. Available from: https://www.tandfonline.com/doi/abs/10.1080/02786826.2020.1726867

26. Zhang Y, Forrister H, Liu J, Dibb J, Anderson B, Schwarz JP, et al. Top-of-atmosphere radiative forcing affected by brown carbon in the upper troposphere. Nat Geosci [Internet]. Nature Publishing Group; 2017;10:486. Available from: http://dx.doi.org/10.1038/ngeo2960

27. Xie C, Xu W, Wang J, Wang Q, Liu D, Tang G, et al. Vertical characterization of aerosol optical

properties and brown carbon in winter in urban Beijing, China. Atmos Chem Phys [Internet]. 2019;19:165–79. Available from: https://www.atmos-chem-phys.net/19/165/2019/

28. Yan J, Wang X, Gong P, Wang C, Cong Z. Review of brown carbon aerosols: Recent progress and perspectives. Sci Total Environ [Internet]. 2018;634:1475–85. Available from: http://www.sciencedirect.com/science/article/pii/S0048969718312476

29. Bond TC, Doherty SJ, Fahey DW, Forster PM, Berntsen T, DeAngelo BJ, et al. Bounding the role of black carbon in the climate system: A scientific assessment. J Geophys Res Atmos [Internet]. 2013 [cited 2013 Aug 8];118:5380–552. Available from: http://doi.wiley.com/10.1002/jgrd.50171

30. Washenfelder RA, Attwood AR, Brock CA, Guo H, L. X, Weber RJ, et al. Biomass burning dominates brown carbon absorption in the rural southeastern United States. Geophys Res Lett [Internet]. 42:653–64. Available from: https://agupubs.onlinelibrary.wiley.com/doi/abs/10.1002/2014GL062444

31. Wang Y, Hu M, Lin P, Guo Q, Wu Z, Li M, et al. Molecular Characterization of Nitrogen-Containing Organic Compounds in Humic-like Substances Emitted from Straw Residue Burning. Environ Sci Technol [Internet]. American Chemical Society; 2017;51:5951–61. Available from: https://doi.org/10.1021/acs.est.7b00248

32. Wang X, Heald CL, Sedlacek AJ, de Sá SS, Martin ST, Alexander ML, et al. Deriving brown carbon from multiwavelength absorption measurements: method and application to AERONET and Aethalometer observations. Atmos Chem Phys [Internet]. 2016;16:12733–52. Available from: https://www.atmos-chem-phys.net/16/12733/2016/

33. Yan C, Zheng M, Bosch C, Andersson A, Desyaterik Y, Sullivan AP, et al. Important fossil source contribution to brown carbon in Beijing during winter. Sci Rep [Internet]. 2017;7:43182. Available from: https://doi.org/10.1038/srep43182

34. Corbin JC, Pieber SM, Czech H, Zanatta M, Jakobi G, Massabò D, et al. Brown and Black Carbon Emitted by a Marine Engine Operated on Heavy Fuel Oil and Distillate Fuels: Optical Properties, Size Distributions, and Emission Factors. J Geophys Res Atmos [Internet]. 2018;123:6175–95. Available from: https://agupubs.onlinelibrary.wiley.com/doi/abs/10.1029/2017JD027818

35. Chen Y, Bond TC. Light absorption by organic carbon from wood combustion. Atmos Chem Phys. 2010;10:1773–87.

36. Storey JME, Curran SJ, Lewis SA, Barone TL, Dempsey AB, Moses-DeBusk M, et al. Evolution and current understanding of physicochemical characterization of particulate matter from reactivity controlled compression ignition combustion on a multicylinder light-duty engine. Int J Engine Res [Internet]. SAGE Publications; 2016;18:505–19. Available from: https://doi.org/10.1177/1468087416661637

37. Prikhodko VY, Curran SJ, Barone TL, Lewis SA, Storey JM, Cho K, et al. Diesel Oxidation Catalyst Control of Hydrocarbon Aerosols From Reactivity Controlled Compression Ignition Combustion [Internet]. 2011. p. 273–8. Available from: http://dx.doi.org/10.1115/IMECE2011-64147

38. Zhong M, Jang M. Light absorption coefficient measurement of SOA using a UV–Visible spectrometer connected with an integrating sphere. Atmos Environ [Internet]. Elsevier Ltd; 2011 [cited 2012 Dec 17];45:4263–71. Available from: http://linkinghub.elsevier.com/retrieve/pii/S1352231011004717

39. Dingle JH, Zimmerman S, Frie AL, Min J, Jung H, Bahreini R. Complex refractive index, single scattering albedo, and mass absorption coefficient of secondary organic aerosols generated from oxidation of biogenic and anthropogenic precursors. Aerosol Sci Technol [Internet]. Taylor & Francis; 2019;53:449–63. Available from: https://doi.org/10.1080/02786826.2019.1571680

40. Lambe AT, Cappa CD, Massoli P, Onasch TB, Forestieri SD, Martin AT, et al. Relationship between oxidation level and optical properties of secondary organic aerosol. Environ Sci Technol [Internet]. 2013;47:6349–57. Available from: http://www.ncbi.nlm.nih.gov/pubmed/23701291

41. Updyke KM, Nguyen TB, Nizkorodov S a. Formation of brown carbon via reactions of ammonia with secondary organic aerosols from biogenic and anthropogenic precursors. Atmos Environ [Internet]. Elsevier Ltd; 2012 [cited 2013 Aug 30];63:22–31. Available from: http://linkinghub.elsevier.com/retrieve/pii/S1352231012008710

42. He Q, Bluvshtein N, Segev L, Meidan D, Flores JM, Brown SS, et al. Evolution of the Complex Refractive Index of Secondary Organic Aerosols during Atmospheric Aging. Environ Sci Technol [Internet]. American Chemical Society; 2018;52:3456–65. Available from: https://doi.org/10.1021/acs.est.7b05742

43. Flores JM, Washenfelder RA, Adler G, Lee HJ, Segev L, Laskin J, et al. Complex refractive indices in the near-ultraviolet spectral region of biogenic secondary organic aerosol aged with ammonia. Phys Chem Chem Phys [Internet]. The Royal Society of Chemistry; 2014;16:10629–42. Available from: http://dx.doi.org/10.1039/C4CP01009D

44. Lee HJ, Aiona PK, Laskin A, Laskin J, Nizkorodov S a. Effect of solar radiation on the optical properties and molecular composition of laboratory proxies of atmospheric brown carbon. Environ Sci Technol. 2014;48:10217–26.

45. De Haan DO, Hawkins LN, Welsh HG, Pednekar R, Casar JR, Pennington EA, et al. Brown Carbon Production in Ammonium- or Amine-Containing Aerosol Particles by Reactive Uptake of Methylglyoxal and Photolytic Cloud Cycling. Environ Sci Technol [Internet]. American Chemical Society; 2017;51:7458–66. Available from: https://doi.org/10.1021/acs.est.7b00159

46. Kampf CJ, Filippi A, Zuth C, Hoffmann T, Opatz T. Secondary brown carbon formation via the dicarbonyl imine pathway: nitrogen heterocycle formation and synergistic effects. Phys Chem Chem Phys [Internet]. The Royal Society of Chemistry; 2016;18:18353–64. Available from: http://dx.doi.org/10.1039/C6CP03029G

47. Lin P, Laskin J, Nizkorodov SA, Laskin A. Revealing Brown Carbon Chromophores Produced in Reactions of Methylglyoxal with Ammonium Sulfate. Environ Sci Technol [Internet]. American Chemical Society; 2015;49:14257–66. Available from: https://doi.org/10.1021/acs.est.5b03608

48. Marrero-Ortiz W, Hu M, Du Z, Ji Y, Wang Y, Guo S, et al. Formation and Optical Properties of Brown Carbon from Small α-Dicarbonyls and Amines. Environ Sci Technol [Internet]. American Chemical Society; 2019;53:117–26. Available from: https://doi.org/10.1021/acs.est.8b03995

49. Haynes JP, Miller KE, Majestic BJ. Investigation into Photoinduced Auto-Oxidation of Polycyclic Aromatic Hydrocarbons Resulting in Brown Carbon Production. Environ Sci Technol [Internet]. American Chemical Society; 2019;53:682–91. Available from: https://doi.org/10.1021/acs.est.8b05704

50. Gilardoni S, Massoli P, Paglione M, Giulianelli L, Carbone C, Rinaldi M, et al. Direct observation of

aqueous secondary organic aerosol from biomass-burning emissions. Proc Natl Acad Sci [Internet]. National Academy of Sciences; 2016;113:10013–8. Available from: https://www.pnas.org/content/113/36/10013

51. Phillips SM, Smith GD. Light Absorption by Charge Transfer Complexes in Brown Carbon Aerosols. Environ Sci Technol Lett. 2014;382–6.

52. Bohren CF, Huffman DR. Absorption and scattering of light by small particles [Internet]. Bohren CF, Huffman DR, editors. Res. Support. by Univ. Arizona Inst. Occup. Environ. Heal. New York WileyInterscience 1983 541 p. Wiley; 1983. Available from: http://adsabs.harvard.edu/abs/1983uaz..rept.....B

53. Li C, He Q, Schade J, Passig J, Zimmermann R, Meidan D, et al. Dynamic changes in optical and chemical properties of tar ball aerosols by atmospheric photochemical aging. Atmos Chem Phys [Internet]. 2019;19:139–63. Available from: https://www.atmos-chem-phys.net/19/139/2019/

54. Sengupta D, Samburova V, Bhattarai C, Kirillova E, Mazzoleni L, Iaukea-Lum M, et al. Light absorption by polar and non-polar aerosol compounds from laboratory biomass combustion. Atmos Chem Phys [Internet]. 2018;18:10849–67. Available from: https://www.atmos-chem-phys.net/18/10849/2018/

55. Liu PF, Abdelmalki N, Hung H-M, Wang Y, Brune WH, Martin ST. Ultraviolet and visible complex refractive indices of secondary organic material produced by photooxidation of the aromatic compounds toluene and m-xylene. Atmos Chem Phys [Internet]. 2015;15:1435–46. Available from: https://www.atmos-chem-phys.net/15/1435/2015/

56. Zhong M, Jang M. Light absorption coefficient measurement of SOA using a UV–Visible spectrometer connected with an integrating sphere. Atmos Environ [Internet]. 2011;45:4263–71. Available from: http://www.sciencedirect.com/science/article/pii/S1352231011004717

57. Li X, Chen Y, Bond TC. Light absorption of organic aerosol from pyrolysis of corn stalk. Atmos Environ [Internet]. Elsevier Ltd; 2016;144:249–56. Available from: http://dx.doi.org/10.1016/j.atmosenv.2016.09.006

58. Chakrabarty RK, Gyawali M, Yatavelli RLN, Pandey A, Watts AC, Knue J, et al. Brown carbon aerosols from burning of boreal peatlands: Microphysical properties, emission factors, and implications for direct radiative forcing. Atmos Chem Phys. 2016;16:3033–40.

59. Sumlin BJ, Heinson YW, Shetty N, Pandey A, Pattison RS, Baker S, et al. UV–Vis–IR spectral complex refractive indices and optical properties of brown carbon aerosol from biomass burning. J Quant Spectrosc Radiat Transf [Internet]. 2018;206:392–8. Available from: http://www.sciencedirect.com/science/article/pii/S0022407317307586

60. Sumlin BJ, Oxford CR, Seo B, Pattison RR, Williams BJ, Chakrabarty RK. Density and Homogeneous Internal Composition of Primary Brown Carbon Aerosol. Environ Sci Technol [Internet]. American Chemical Society; 2018;52:3982–9. Available from: https://doi.org/10.1021/acs.est.8b00093

61. Kirchstetter TW, Novakov T, Hobbs P V. Evidence that the spectral dependence of light absorption by aerosols is affected by organic carbon. J Geophys Res. 2004;109:D21208.

62. Bond TC, Bergstrom RW. Light Absorption by Carbonaceous Particles: An Investigative Review. Aerosol Sci Technol [Internet]. 2005 [cited 2012 Oct 31];39:1–41. Available from:

http://www.tandfonline.com/doi/abs/10.1080/02786820500421521

63. Lu Z, Streets DG, Winijkul E, Yan F, Chen Y, Bond TC, et al. Light Absorption Properties and Radiative Effects of Primary Organic Aerosol Emissions. Environ Sci Technol [Internet]. 2015;DOI: 10.1021/acs.est.5b00211. Available from: http://pubs.acs.org/doi/abs/10.1021/acs.est.5b00211

64. Dinar E, Abo Riziq a., Spindler C, Erlick C, Kiss G, Rudich Y. The complex refractive index of atmospheric and model humic-like substances (HULIS) retrieved by a cavity ring down aerosol spectrometer (CRD-AS). Faraday Discuss [Internet]. 2008 [cited 2013 Aug 13];137:279. Available from: http://xlink.rsc.org/?DOI=b703111d

65. Di Lorenzo RA, Washenfelder RA, Attwood AR, Guo H, Xu L, Ng NL, et al. Molecular-Size-Separated Brown Carbon Absorption for Biomass-Burning Aerosol at Multiple Field Sites. Environ Sci Technol. 2017;51:3128–37.

66. Wu G-M, Cong Z-Y, Kang S-C, Kawamura K, Fu P-Q, Zhang Y-L, et al. Brown carbon in the cryosphere: Current knowledge and perspective. Adv Clim Chang Res [Internet]. 2016;7:82–9. Available from: http://www.sciencedirect.com/science/article/pii/S1674927816300302

67. Shetty NJ, Pandey A, Baker S, Hao WM, Chakrabarty RK. Measuring light absorption by freshly emitted organic aerosols: optical artifacts in traditional solvent-extraction-based methods. Atmos Chem Phys [Internet]. 2019;19:8817–30. Available from: https://www.atmos-chem-phys.net/19/8817/2019/

68. Zaveri RA, Easter RC, Fast JD, Peters LK. Model for Simulating Aerosol Interactions and Chemistry (MOSAIC). J Geophys Res Atmos. 2008;113:D13.

69. Donahue NM, Epstein SA, Pandis SN, Robinson AL. A two-dimensional volatility basis set: 1. organic-aerosol mixing thermodynamics. Atmos Chem Phys. 2011;11:3303–18.

70. Pósfai M. Atmospheric tar balls: Particles from biomass and biofuel burning. J Geophys Res [Internet]. 2004 [cited 2012 Nov 1];109:1–9. Available from: http://www.agu.org/pubs/crossref/2004/2003JD004169.shtml

71. Adachi K, Sedlacek AJ, Kleinman L, Chand D, Hubbe JM, Buseck PR. Volume changes upon heating of aerosol particles from biomass burning using transmission electron microscopy. Aerosol Sci Technol [Internet]. Taylor & Francis; 2018;52:46–56. Available from: https://doi.org/10.1080/02786826.2017.1373181

72. Adachi K, Sedlacek AJ, Kleinman L, Springston SR, Wang J, Chand D, et al. Spherical tarball particles form through rapid chemical and physical changes of organic matter in biomass-burning smoke. Proc Natl Acad Sci [Internet]. National Academy of Sciences; 2019;116:19336–41. Available from: https://www.pnas.org/content/116/39/19336

73. Sedlacek III AJ, Buseck PR, Adachi K, Onasch TB, Springston SR, Kleinman L. Formation and evolution of tar balls from northwestern US wildfires. Atmos Chem Phys [Internet]. 2018;18:11289–301. Available from: https://www.atmos-chem-phys.net/18/11289/2018/

74. Tóth Á, Hoffer A, Pósfai M, Ajtai T, Kónya Z, Blazsó M, et al. Chemical characterization of laboratory-generated tar ball particles. Atmos Chem Phys [Internet]. 2018;18:10407–18. Available from: https://www.atmos-chem-phys.net/18/10407/2018/

75. Hoffer A, Tóth A, Nyirő-Kósa I, Pósfai M, Gelencsér A. Light absorption properties of laboratory-generated\hack{\break} tar ball particles. Atmos Chem Phys [Internet]. 2016;16:239–46. Available from: https://www.atmos-chem-phys.net/16/239/2016/

76. Hoffer A, Tóth Á, Pósfai M, Chung CE, Gelencsér A. Brown carbon absorption in the red and near-infrared spectral region. Atmos Meas Tech [Internet]. 2017;10:2353–9. Available from: https://www.atmos-meas-tech.net/10/2353/2017/

77. Claeys M, Vermeylen R, Yasmeen F, Gómez-González Y, Chi X, Maenhaut W, et al. Chemical characterisation of humic-like substances from urban, rural and tropical biomass burning environments using liquid chromatography with UV/vis photodiode array detection and electrospray ionisation mass spectrometry. Environ Chem [Internet]. 2012;9:273–84. Available from: https://doi.org/10.1071/EN11163

78. Hoffer A, Gelencsér A, Guyon P, Kiss G, Schmid O, Frank GP, et al. Optical properties of humic-like substances (HULIS) in biomass-burning aerosols. Atmos Chem Phys [Internet]. 2006;6:3563–70. Available from: https://www.atmos-chem-phys.net/6/3563/2006/

79. Utry N, Ajtai T, Filep Á, Dániel Pintér M, Hoffer A, Bozoki Z, et al. Mass specific optical absorption coefficient of HULIS aerosol measured by a four-wavelength photoacoustic spectrometer at NIR, VIS and UV wavelengths. Atmos Environ [Internet]. 2013;69:321–4. Available from: http://www.sciencedirect.com/science/article/pii/S1352231013000095

80. Kwon D, Sovers MJ, Grassian VH, Kleiber PD, Young MA. Optical Properties of Humic Material Standards: Solution Phase and Aerosol Measurements. ACS Earth Sp Chem [Internet]. American Chemical Society; 2018;2:1102–11. Available from: https://doi.org/10.1021/acsearthspacechem.8b00097

81. Akagi SK, Yokelson RJ, Wiedinmyer C, Alvarado MJ, Reid JS, Karl T, et al. Emission factors for open and domestic biomass burning for use in atmospheric models. Atmos Chem Phys [Internet]. 2011;11:4039–72. Available from: http://www.atmos-chem-phys.net/11/4039/2011/

82. Pokhrel RP, Wagner NL, Langridge JM, Lack D a., Jayarathne T, Stone E a., et al. Parameterization of single-scattering albedo (SSA) and absorption Ångström exponent (AAE) with EC/OC for aerosol emissions from biomass burning. Atmos Chem Phys. 2016;16:9549–61.

83. McMeeking GR, Fortner E, Onasch TB, Taylor JW, Flynn M, Coe H, et al. Impacts of nonrefractory material on light absorption by aerosols emitted from biomass burning. J Geophys Res Atmos [Internet]. 2014;119:12,212-272,286. Available from: https://agupubs.onlinelibrary.wiley.com/doi/abs/10.1002/2014JD021750

84. Hammer MS, Martin R V, van Donkelaar A, Buchard V, Torres O, Ridley DA, et al. Interpreting the ultraviolet aerosol index observed with the OMI satellite instrument to understand absorption by organic aerosols: implications for atmospheric oxidation and direct radiative effects. Atmos Chem Phys [Internet]. 2016;16:2507–23. Available from: https://www.atmos-chem-phys.net/16/2507/2016/

85. Michelsen HA. Probing soot formation , chemical and physical evolution , and oxidation : A review of in situ diagnostic techniques and needs. Proc Combust Inst [Internet]. Elsevier Inc.; 2017;36:717–35. Available from: http://dx.doi.org/10.1016/j.proci.2016.08.027

86. Johansson KO, El Gabaly F, Schrader PE, Campbell MF, Michelsen HA. Evolution of maturity levels of

the particle surface and bulk during soot growth and oxidation in a flame. Aerosol Sci Technol [Internet]. Taylor & Francis; 2017;51:1333–44. Available from: https://doi.org/10.1080/02786826.2017.1355047

87. Johansson KO, Head-Gordon MP, Schrader PE, Wilson KR, Michelsen HA. Resonance-stabilized hydrocarbon-radical chain reactions may explain soot inception and growth. Science (80-) [Internet]. 2018;361:997. Available from: http://science.sciencemag.org/content/361/6406/997.abstract

88. Wiedinmyer C, Akagi SK, Yokelson RJ, Emmons LK, Al-Saadi J a., Orlando JJ, et al. The Fire INventory from NCAR (FINN): a high resolution global model to estimate the emissions from open burning. Geosci Model Dev [Internet]. 2011 [cited 2013 Aug 6];4:625–41. Available from: http://www.geosci-model-dev.net/4/625/2011/

89. Li H, McMeeking GR, May AA. Development of a Universal Correction Algorithm for Filter-Based Absorption Photometers. Atmos Meas Tech Discuss [Internet]. 2019;2019:1–32. Available from: https://www.atmos-meas-tech-discuss.net/amt-2019-336/

90. Fischer A, Smith GD. A Portable, Four-wavelength, Single-cell Photoacoustic Spectrometer for Ambient Aerosol Absorption. Aerosol Sci Technol. 2017;

91. Fischer DA, Smith GD. Can ozone be used to calibrate aerosol photoacoustic spectrometers? Atmos Meas Tech [Internet]. 2018;11:6419–27. Available from: https://www.atmos-meas-tech.net/11/6419/2018/

92. Bluvshtein N, Flores JM, He Q, Segre E, Segev L, Hong N, et al. Calibration of a multi-pass photoacoustic spectrometer cell using light-absorbing aerosols. Atmos Meas Tech [Internet]. 2017;10:1203–13. Available from: https://www.atmos-meas-tech.net/10/1203/2017/

93. Foster K, Pokhrel R, Burkhart M, Murphy S. A novel approach to calibrating a photoacoustic absorption spectrometer using polydisperse absorbing aerosol. Atmos Meas Tech [Internet]. 2019;12:3351–63. Available from: https://www.atmos-meas-tech.net/12/3351/2019/

94. Liu D, Taylor JW, Young DE, Flynn MJ, Coe H, Allan JD. The effect of complex black carbon microphysics on the determination of the optical properties of brown carbon. Geophys Res Lett. 2015;42:613–9.

95. Stevens R, Dastoor A. A Review of the Representation of Aerosol Mixing State in Atmospheric Models. Atmosphere (Basel) [Internet]. 2019;10. Available from: https://www.mdpi.com/2073-4433/10/4/168

96. Wong JPS, Tsagkaraki M, Tsiodra I, Mihalopoulos N, Violaki K, Kanakidou M, et al. Atmospheric evolution of molecular-weight-separated brown carbon from biomass burning. Atmos Chem Phys [Internet]. 2019;19:7319–34. Available from: https://www.atmos-chem-phys.net/19/7319/2019/

97. Hems RF, Abbatt JPD. Aqueous Phase Photo-oxidation of Brown Carbon Nitrophenols: Reaction Kinetics, Mechanism, and Evolution of Light Absorption. ACS Earth Sp Chem [Internet]. American Chemical Society; 2018;2:225–34. Available from: https://doi.org/10.1021/acsearthspacechem.7b00123

98. Zhao R, Lee AKY, Huang L, Li X, Yang F, Abbatt JPD. Photochemical processing of aqueous atmospheric brown carbon. Atmos Chem Phys [Internet]. 2015;15:6087–100. Available from: https://www.atmos-chem-phys.net/15/6087/2015/

99. Keyte IJ, Harrison RM, Lammel G. Chemical reactivity and long-range transport potential of polycyclic aromatic hydrocarbons – a review. Chem Soc Rev [Internet]. The Royal Society of Chemistry; 2013;42:9333–91. Available from: http://dx.doi.org/10.1039/C3CS60147A

100. Bluvshtein N, Lin P, Flores JM, Segev L, Mazar Y, Tas E, et al. Broadband optical properties of biomass-burning aerosol and identification of brown carbon chromophores. J Geophys Res Atmos [Internet]. 2017;122:5441–56. Available from: https://agupubs.onlinelibrary.wiley.com/doi/abs/10.1002/2016JD026230

101. Wang Q, Saturno J, Chi X, Walter D, Lavric J V., Moran- Zuloaga D, et al. Modeling investigation of light absorbing aerosols in the central Amazon during the wet season. Atmos Chem Phys [Internet]. 2016;16:14775–94. Available from: http://www.atmos-chem-phys-discuss.net/acp-2016-586/

102. Park RJ, Kim MJ, Jeong JI, Youn D, Kim S. A contribution of brown carbon aerosol to the aerosol light absorption and its radiative forcing in East Asia. Atmos Environ [Internet]. 2010;44:1414–21. Available from: http://www.sciencedirect.com/science/article/pii/S1352231010001019

103. Feng Y, Ramanathan V, Kotamarthi VR. Brown carbon: a significant atmospheric absorber of solar radiation? Atmos Chem Phys [Internet]. 2013 [cited 2013 Sep 17];13:8607–21. Available from: http://www.atmos-chem-phys.net/13/8607/2013/

104. Lin G, Penner JE, Flanner MG, Sillman S, Xu L, Zhu C. Radiative forcing of organic aerosol in the atmosphere and on snow: Effects of SOA and brown carbon. J Geophys Res Atmos. 2014;

105. Jacobson MZ. Effects of biomass burning on climate, accounting for heat and moisture fluxes, black and brown carbon, and cloud absorption effects. J Geophys Res. 2014;119:8980–9002.

106. Saleh R, Marks M, Heo J, Adams PJ, Donahue NM, Robinson AL. Contribution of brown carbon and lensing to the direct radiative effect of carbonaceous aerosols from biomass and biofuel burning emissions. J Geophys Res Atmos. 2015;

107. Jo DS, Park RJ, Lee S, Kim S-W, Zhang X. A global simulation of brown carbon: implications for photochemistry and direct radiative effect. Atmos Chem Phys [Internet]. 2016;16:3413–32. Available from: https://www.atmos-chem-phys.net/16/3413/2016/

108. Brown H, Liu X, Feng Y, Jiang Y, Wu M, Lu Z, et al. Radiative effect and climate impacts of brown carbon with the Community Atmosphere Model (CAM5). Atmos Chem Phys [Internet]. 2018;18:17745–68. Available from: https://www.atmos-chem-phys.net/18/17745/2018/

109. Wang X, Heald CL, Ridley D a., Schwarz JP, Spackman JR, Perring a. E, et al. Exploiting simultaneous observational constraints on mass and absorption to estimate the global direct radiative forcing of black carbon and brown carbon. Atmos Chem Phys Discuss [Internet]. 2014 [cited 2014 Aug 11];14:17527–83. Available from: http://www.atmos-chem-phys-discuss.net/14/17527/2014/

110. Wang X, Heald CL, Liu J, Weber RJ, Campuzano-Jost P, Jimenez JL, et al. Exploring the observational constraints on the simulation of brown carbon. Atmos Chem Phys [Internet]. 2018;18:635–53. Available from: https://www.atmos-chem-phys.net/18/635/2018/

111. Wiedinmyer C, Akagi SK, Yokelson RJ, Emmons LK, Al-Saadi JA, Orlando JJ, et al. The Fire INventory from NCAR (FINN): a high resolution global model to estimate the emissions from open burning. Geosci Model Dev [Internet]. 2011;4:625–41. Available from: https://www.geosci-model-dev.net/4/625/2011/

112. van der Werf GR, Randerson JT, Giglio L, van Leeuwen TT, Chen Y, Rogers BM, et al. Global fire emissions estimates during 1997--2016. Earth Syst Sci Data [Internet]. 2017;9:697–720. Available from: https://www.earth-syst-sci-data.net/9/697/2017/

113. Holder AL, Hagler GSW, Aurell J, Hays MD, Gullett BK. Particulate matter and black carbon optical properties and emission factors from prescribed fires in the southeastern United States. J Geophys Res Atmos [Internet]. 2016;121:3465–83. Available from: https://agupubs.onlinelibrary.wiley.com/doi/abs/10.1002/2015JD024321

114. Toon OB, Maring H, Dibb J, Ferrare R, Jacob DJ, Jensen EJ, et al. Planning, implementation, and scientific goals of the Studies of Emissions and Atmospheric Composition, Clouds and Climate Coupling by Regional Surveys (SEAC4RS) field mission. J Geophys Res Atmos [Internet]. 2016;121:4967–5009. Available from: https://agupubs.onlinelibrary.wiley.com/doi/abs/10.1002/2015JD024297

115. Zhang XL, Lin YH, Surratt JD, Weber RJ. Sources, Composition and Absorption Ångström Exponent of Light absorbing Organic Components in Aerosol Extracts from the Los Angeles Basin. Environ Sci Technol. 2013;47:3685–3693.

116. Liu J, Bergin M, Guo H, King L, Kotra N, Edgerton E, et al. Size-resolved measurements of brown carbon in water and methanol extracts and estimates of their contribution to ambient fine-particle light absorption. Atmos Chem Phys. 2013;13:12389–12404.

117. McMeeking GR. The Optical, Chemical, And Physical Properties Of Aerosols And Gases Emitted By The Laboratory Combustion Of Wildland Fuels. Colorado State University; 2008.

118. Nakayama T, Matsumi Y, Sato K, Imamura T, Yamazaki A, Uchiyama A. Laboratory studies on optical properties of secondary organic aerosols generated during the photooxidation of toluene and the ozonolysis of α -pinene. J Geophys Res [Internet]. 2010 [cited 2012 Oct 31];115:1–11. Available from: http://www.agu.org/pubs/crossref/2010/2010JD014387.shtml